

# EMOTION AND ACOUSTICS SHOULD AGREE: CROSS-LEVEL INCONSISTENCY ANALYSIS FOR AUDIO DEEPFAKE DETECTION

Jinhua Zhang      Zhenqi Jia      Rui Liu<sup>†</sup>

Inner Mongolia University

zjh\_imu@163.com, jiazhenqi7@163.com, liurui\_imu@163.com

## ABSTRACT

Audio Deepfake Detection (ADD) aims to detect spoof speech from bonafide speech. Most prior studies assume that stronger correlations within or across acoustic and emotional features imply authenticity, and thus focus on enhancing or measuring such correlations. However, existing methods often treat acoustic and emotional features in isolation or rely on correlation metrics, which overlook subtle desynchronization between them and smooth out abrupt discontinuities. To address these issues, we propose EAI-ADD, which treats cross-level emotion–acoustic inconsistency as the primary detection signal. We first project emotional and acoustic representations into a comparable space. Then we progressively integrating frame- and utterance-level emotion features with acoustic features to capture cross-level emotion–acoustic inconsistencies across different temporal granularities. Experimental results on the ASVspoof 2019LA and 2021LA datasets demonstrate that the proposed EAI-ADD outperforms baselines, providing a more effective solution for audio anti-spoofing detection. The source code and demos are available at: <https://github.com/AI-S2-Lab/EAI-ADD>.

**Index Terms**— Audio Deepfake Detection, Hierarchical Inconsistency Graph, Emotion–Acoustic Inconsistency, Emotion–Acoustic Alignment

## 1. INTRODUCTION

Audio Deepfake Detection (ADD) aims to determine whether an audio sample is bonafide or spoof and is attracting growing interest [1, 2, 3]. Recent work leverages large audio models such as WavLM to obtain finegrained acoustic representations [4]. Some emotion-driven approaches primarily focus on utterance-level emotions and their correlations with other features [5, 6].

<sup>†</sup> denotes the corresponding author. This research was funded by the General Program(No.62476146) of the National Natural Science Foundation of China, the Young Elite Scientists Sponsorship Program by CAST(2024QNRC001), the Outstanding Youth Project of Inner Mongolia Natural Science Foundation(2025JQ011), the Key R&D and Achievement Transformation Program of Inner Mongolia Autonomous Region(2025YFHH0014), and the Central Government Fund for Promoting Local Scientific and Technological Development(2025ZY0143).

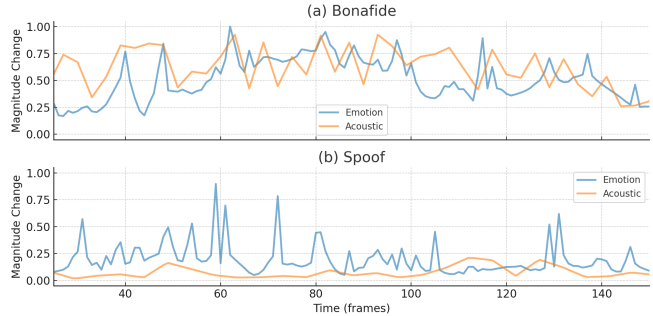


**Fig. 1.** Frame-level change magnitudes of emotion and acoustic features.

Existing ADD works have largely analyzed patterns within individual acoustic or emotional features [4, 7, 8], or measured how strongly the two are correlated [6], using such correlations as cues to judge authenticity. However, in natural speech, emotional dynamics evolve smoothly over time and remain tightly aligned with the underlying acoustic structure [9, 10, 11]. For example, a gradual increase in emotional arousal is usually accompanied by consistent variations in acoustic representations, whereas synthetic speech often shows prosody–emotion desynchronization, such as abrupt acoustic fluctuations without matching emotional changes [12, 13]. As shown in Fig. 1, we use the L2 distance<sup>1</sup> [14] to compute the frame-level change magnitudes of the emotion features and the acoustic features, and normalize them to [0, 1] for comparison on the same scale. In bonafide speech (Fig. 1(a)), the two curves co-vary over long stretches, indicating that acoustic fluctuations tend to co-vary with emotional dynamics over time. In contrast, spoof speech (Fig. 1(b)) exhibits clear desynchronization: sharp bursts in the emotion curve are not accompanied by corresponding acoustic changes (and vice versa). Pearson correlations over 300 randomly selected samples also show more stable distributions for bonafide speech and greater inconsistency for spoof speech. This difference in alignment patterns serves as the key cues of spoof speech. Existing correlation-based analyses tend to smooth over or miss these subtle misalignments,

<sup>1</sup>L2 distance is chosen because it measures the magnitude rather than the direction of frame-level changes, making it well-suited to our task objective.

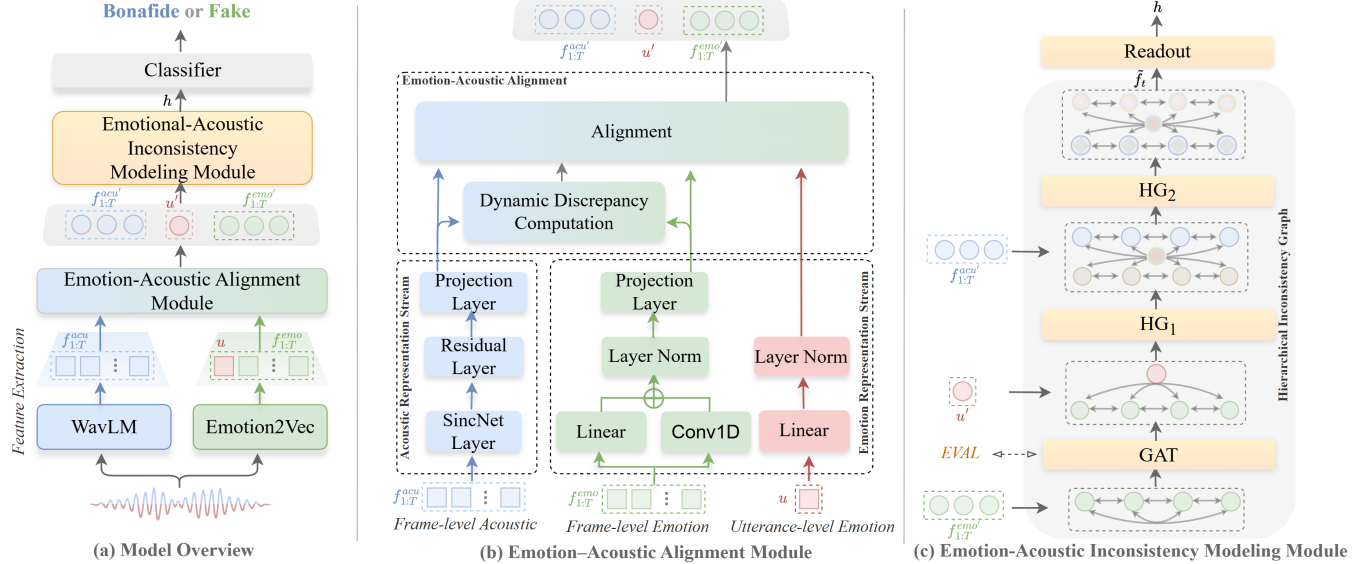


**Fig. 2.** Our overall framework is illustrated in (a). (b) illustrates the Emotion-Acoustic Alignment Module. (c) depicts Emotion-Acoustic Inconsistency Modeling Module.

treating them as statistical noise. We therefore shift the focus: rather than seeking correlation as a proxy for authenticity, we explicitly model mismatches between emotional dynamics and acoustic patterns as direct and discriminative cues, on the premise that such mismatches are rare in bonafide speech but prevalent in spoof audio.

To this end, this paper proposes a novel Emotion-Acoustic Inconsistency framework for ADD, termed **EAI-ADD**, that aims to uncover spoofing artifacts by modeling the inconsistency between emotional evolution and acoustic structural features. Specifically, we introduce an Emotion-Acoustic Alignment Module to project emotional and acoustic features into a unified representation space. On top of this alignment, the Emotion-Acoustic Inconsistency Modeling Module enforces reliable cross-level emotion-acoustic inconsistency analysis by integrating a Emotional Variation Amplification Loss to refine frame-level emotion trajectories and a Hierarchical Emotion-Acoustic Graph to link frame-/utterance-level emotional and frame-level acoustic nodes for detecting inconsistency patterns. Experiments on the ASVspoof 2019 LA database demonstrate that our method consistently outperforms strong baselines. As far as we know, this is the first ADD study to explicitly model emotion-acoustic inconsistency as the key evidence for spoof detection.

## 2. EAI-ADD NEURAL ARCHITECTURE

We present EAI-ADD (Fig. 2), which consists of Feature Extraction Process, Emotion-Acoustic Alignment Module (EAAM), Emotion-Acoustic Inconsistency Modeling Module (EAIMM) and a Binary Classifier. The Feature Extraction process generates frame-/utterance-level emotional features and frame-level acoustic features. EAAM projects

emotional and acoustic representations into a unified space. EAIMM enforces cross-level emotional inconsistency, capturing both short-term irregularities and cross-scale inconsistencies indicative of spoofing. The classifier produces the final bonafide/spoof decision.

### 2.1. Feature Extraction

We adopt WavLM to extract acoustic features for its stronger temporal-context modeling and fine-grained representations on short utterances compared with Wav2Vec2.0 [15] and HuBERT [16], and we fine-tune it with AASIST [17] for ADD by freezing lower layers and adapting upper layers to obtain task-relevant representations for accurate detection. We use frame-level acoustic features to capture subtle local anomalies, while utterance-level acoustic features are not used because global pooling may obscure such fine-grained discrepancies. Emotion2vec [18] provides frame-/utterance-level emotional features. Its contrastive, context-aware pre-training effectively captures inter-frame emotional dynamics and yields superior emotion metrics such as lower MSE, making it well suited for our task. Frame-level emotion features reflect detailed dynamics, whereas utterance-level emotion features serve as contextual weights to aggregate and guide frame-level emotion differences, thereby providing a global reference for local emotional evolution.

### 2.2. Emotion-Acoustic Alignment Module

This module processes emotional and acoustic features through dedicated streams to mitigate redundancy while preserving key variation information, then projecting them into a unified representation.

**Acoustic Representation Stream (ARS).** This stream processes frame-level acoustic features  $f_{1:T}^{acu} \in \mathbb{R}^{T \times d}$ , focusing on compact representation without losing essential cues. Here,  $f_{1:T}^{acu}$  denotes the sequence matrix formed by stacking the updated frame vectors  $f_t^{acu}$ . The SincNet layer, designed as a parameterized band-pass 1D convolution, focuses on enhancing discriminative frequency components embedded in the acoustic representations. The residual block then captures short-term dependencies and local fluctuations, safeguarding fine-grained acoustic dynamics. Finally, a projection layer maps the features into a representation space compatible with emotion embeddings, providing stable inputs for alignment.

**Emotion Representation Stream (ERS).** This stream processes the frame-/utterance-level emotion features  $f_{1:T}^{emo} \in \mathbb{R}^{T \times d}$  and  $u \in \mathbb{R}^{1 \times d}$ , preserving emotional information at different granularities. Here,  $f_{1:T}^{emo}$  denotes the sequence matrix formed by stacking the updated frame vectors  $f_t^{emo}$ . In the frame-level pathway, the parallel operation of Linear and Conv1D aims to remove redundant information while preserving the ability to capture short-term dependencies and fine-grained emotional variations. The summed output is normalized with LayerNorm and then projected to obtain stable frame-level emotional representations. In the utterance-level pathway, the utterance-level emotion embedding is projected through a linear layer and normalized by LayerNorm, providing a stable representation of the global emotional trend.

**Emotion-Acoustic Alignment.** This part aims to align two kinds of features in a shared representation space: **(1) Dynamic Discrepancy Computation:** At the frame level, we first compute the discrepancy using first-order differences to capture the dynamic variations between consecutive frames over time. Concretely,  $\Delta f_t = f_t^{emo} - f_{t-1}^{emo}$ ,  $\Delta a_t = f_t^{acu} - f_{t-1}^{acu}$ , and construct the frame-level change difference  $d^{fra} = |\Delta f_t - \Delta a_t|$  as the dynamic discrepancy descriptor. For the utterance level, average pooling is applied to the frame-level emotion features  $u$  to match the dimension of the utterance-level embedding  $u^{emo}$ , the global discrepancy is computed as  $d^{utt} = |u - u^{emo}|$ . **(2) Alignment:** The descriptors  $d^{utt}$  and  $d^{fra}$  are fed into a fixed-sign dual-head softmax to produce two complementary weights:  $[\gamma_t^{align}, \gamma_t^{mis}] = \text{softmax}([-d^{fra/utt}, +d^{fra/utt}])$ . Here,  $\gamma_t^{align}$  emphasizes alignment components, while  $\gamma_t^{mis}$  explicitly encodes the degree of temporal inconsistency. During feature updating, each stream selectively incorporates information from the other stream:  $f_t^{emo/acu'} = \gamma_t^{align} \cdot f_t^{emo/acu} + \gamma_t^{mis} \cdot f_t^{acu/emo}$ ,  $u' = \gamma_t^{align} \cdot u + \gamma_t^{mis} \cdot u^{emo}$ . The resulting features  $f_{1:T}^{emo'}$ ,  $u'$ , and  $f_{1:T}^{acu'}$  achieve alignment while retaining their respective fine-grained characteristics, enabling subsequent inconsistency detection.

### 2.3. Emotion-Acoustic Inconsistency Modeling Module

This module enforces reliable cross-level emotion-acoustic inconsistency analysis. EVAL employs contrastive learning

to capture and amplify abnormal jumps in the temporal evolution of frame-level emotions, providing clearer discriminative emotion evolution cues. HIG employs the hierarchical heterogeneous graph modeling to progressively integrating frame- and utterance-level emotion features with acoustic structure features to capture cross-level emotion-acoustic inconsistencies across different temporal granularities.

**Emotional Variation Amplification Loss (EVAL).** EVAL employs contrastive learning to capture and amplify abnormal jumps in the temporal evolution of frame-level emotions, providing clearer discriminative emotion evolution cues. We first compute the temporal difference  $\Delta f_t^{emo}$  between frame  $t$  and its immediate neighbor to characterize the local emotional transition at time  $t$ . To obtain a reference for this transition, we aggregate the temporal differences  $\{\Delta f_j^{emo} \mid j \in \mathcal{N}(t)\}$  from the neighboring frames into a prototype  $g_t$ , where the sentence-level embedding  $u'$  provides contextual weights. Here,  $\mathcal{N}(t) = \{j \mid 0 \leq j \leq T-2, |j-t| \leq k\}$  denotes the set of indices within a temporal window of radius  $k$  around  $t$ , with  $k$  being a predefined window size:

$$g_t = \frac{\sum_{j \in \mathcal{N}(t)} \alpha_{tj} \Delta f_j^{emo}}{\sum_{j \in \mathcal{N}(t)} \alpha_{tj}}, \quad \alpha_{tj} = \exp\left(\frac{u' \cdot f_j^{(1)}}{\tau}\right). \quad (1)$$

Here,  $g_t$  represents the expected local trend of emotional variation under the global guidance of  $u'$ ,  $f_j^{(1)}$  will be introduced in HIG. We then apply a contrastive objective InfoNCE [19] to enforce  $\Delta f_t$  to align with its prototype while being separated from negative samples  $\Delta f^-$ . Specifically, negative samples  $\Delta f^-$  are obtained from two sources within the same utterance: (i) temporal differences between far-apart frames to break short-term continuity; (ii) temporal differences from randomly shuffled frame orders to destroy natural sequential evolution.

**Hierarchical Inconsistency Graph (HIG).** HIG captures cross-level emotion-acoustic inconsistencies by progressively integrating frame- and utterance-level emotion representations with acoustic structure via a multi-stage heterogeneous graph. We first construct a frame-level temporal graph, where each frame node aggregates information from its temporal neighbors via graph attention:

$$\{f_t^{(1)}\}_{t=1}^T = \text{GAT}(f_t^{emo'}, \{f_{t-1}^{emo'}, f_{t+1}^{emo'}\}), \quad t=1, \dots, T. \quad (2)$$

Here,  $f_t^{(1)}$  denotes the frame-level emotion feature after the first-stage GAT update, encoding local temporal context. On top of this, EVAL amplifies abnormal temporal jumps, suppressing natural transitions and preserving salient inconsistency cues. The enhanced frame embeddings are then integrated with the utterance-level emotion node  $u'$  and frame-level acoustic nodes  $w_t$  to form the node set.  $V = \{f_t^{(1)}\}_{t=1}^T \cup u' \cup \{f_t^{acu'}\}_{t=1}^T$ , where the edge set includes  $E_{FF}$ ,  $E_{FU}$ , and  $E_{FS}$ . All cross-level connections are implicitly modeled by graph attention, without manually specified edge rules. The update is performed in two heterogeneous stages: the first stage ( $HG_1$ ) detects local-global emotional

inconsistencies, and the second stage ( $HG_2$ ) detects emotion–acoustic mismatches:

$$\tilde{f}_t = HG_2\left(HG_1\left(\{f_t^{(1)}\}_{t=1}^T, u'\right), \{f_t^{\text{acu}'}\}_{t=1}^T\right) \quad (3)$$

The node-level outputs  $\tilde{f}_t$  are aggregated by the pooling-based Readout, producing a compact graph-level representation  $h$  that is subsequently fed into the binary classifier.

## 2.4. Overall Objective

The final loss combines classification cross-entropy (CE) and EVAL using homoscedastic uncertainty weighting [20]. Let  $s = \log \sigma^2$  be trainable:  $\mathcal{L} = \mathcal{L}_{\text{CE}} + e^{-s} \mathcal{L}_{\text{EVAL}} + s$ , where  $s$  regularizes the weighting to prevent vanishing weights.

## 3. EXPERIMENTS

### 3.1. Experimental Protocol

To ensure consistency with prior work, we evaluate our method on the ASVspoof 2019LA [21] and 2021LA [22] datasets. Performance is evaluated using EER [23] and tDCF [24]. Audio samples are standardized to 64,600 samples. The model has 0.83M parameters, requires 0.34 GFLOPs per utterance, and is trained for 60 epochs using Adam ( $10^{-5}$  learning rate,  $10^{-4}$  weight decay) on an NVIDIA A100 GPU, with results averaged over three random seeds.

### 3.2. Main Results

Table 1 reports the performance of EAI-ADD against existing approaches on the 2019LA evaluation set. EAI-ADD achieves the best results, with a min tDCF of 0.0110 and an EER of 0.34%, reducing tDCF and EER by 4.3% and 15% compared with the strongest baseline. Consistent improvements are also observed on 2021LA, indicating stronger generalization to unseen spoofing conditions. These improvements stem from EAI-ADD’s modeling of emotion–acoustic inconsistency. By aligning emotional and acoustic features and leveraging cross-level graph relations, the model highlights abnormal emotion variations and emotion–acoustic mismatches, maintaining strong discriminative power under unseen attacks and complex distortions.

### 3.3. Ablation Study

Table 2 presents ablation results on the ASVspoof 2019LA evaluation set. **(1) Main Component Ablation.** Removing any core module degrades performance. EAAM removal increases tDCF/EER to 0.0118/0.42%, EVAL removal yields 0.0117/0.41%, and removing HIG causes the largest drop (0.0121/0.44%), underscoring the role of multi-level consistency reasoning. **(2) Alternative Mechanism Variants.** Replacing ARS and ERS with linear projection leads to a clear performance drop (0.0125 / 0.46%), indicating that

**Table 1.** Comparison with other anti-spoofing systems on 2019LA and 2021LA datasets (pooled min tDCF and EER). (– means unreported due to closed source baseline.)

System	2019 LA		2021 LA	
	tDCF (↓)	EER(%) (↓)	tDCF (↓)	EER(%) (↓)
SE-Rawformer [25]	0.0344	1.05	0.3186	4.98
AASIST [17]	0.0275	0.83	0.3398	5.59
DFSyncNet [26]	0.0176	0.52	0.2731	3.38
f0+Res2Net [27]	0.0159	0.47	0.2642	3.61
WavLM+MFA [28]	0.0126	0.42	–	5.08
WavLM+RAD-MFA [29]	0.0115	0.40	–	4.83
<b>EAI-ADD (Ours)</b>	<b>0.0110</b>	<b>0.34</b>	<b>0.2533</b>	<b>3.29</b>

**Table 2.** Ablation study on the 2019LA dataset. The upper block removes key modules, the middle block replaces streams and graph variants, and the lower block studies the effect of temporal window size  $k$  in EVAL.

Setting	tDCF (↓)	EER(%) (↓)
<i>Main Component Ablation</i>		
w/o EAAM	0.0118	0.42
w/o EVAL	0.0117	0.41
w/o HIG	0.0121	0.44
<i>Alternative Mechanism Variants</i>		
ARS&ERS → Linear Projection	0.0125	0.46
GAT → GCN	0.0133	0.52
<i>Hyperparameter Study (<math>k</math> in EVAL)</i>		
$k = 1, 2$	0.0120 / 0.0115	0.43 / 0.39
$k = 3$	<b>0.0110</b>	<b>0.34</b>
$k = 4, 5$	0.0118 / 0.0123	0.41 / 0.46

naive dimensionality reduction fails to capture fine-grained or complementary emotion–acoustic patterns. Similarly, replacing GAT with GCN further degrades performance (0.0133 / 0.52%), which highlights the necessity of adaptive attention-based aggregation for effectively modeling heterogeneous relationships. **(3) Hyperparameter Study ( $k$  in EVAL).** A temporal window size of  $k = 3$  achieves the best performance (0.0110 / 0.34%). Both smaller ( $k = 1, 2$ ) and larger ( $k = 4, 5$ ) windows yield inferior results, indicating that a moderate temporal scope best balances short-term dynamics and noise suppression. Overall, these ablation results confirm that each module is essential. Simplifying ARS/ERS to linear projection or replacing GAT with GCN consistently degrades performance, underscoring the importance of dedicated streams and attention-based message passing for modeling fine-grained and heterogeneous dependencies.

## 4. CONCLUSIONS

This paper presented an ADD framework EAI-ADD that explicitly models emotion–acoustic inconsistency as the primary discriminative cue. The proposed EAAM aligns emotional and acoustic representations within a unified space, while the EAIMM conducts hierarchical inconsistency analysis to capture cross-level discrepancies. Experimental results on two datasets demonstrate that EAI-ADD achieves best performance. Notwithstanding these gains, the approach has yet to be validated under real-time or highly compressed conditions, which will be the focus of future investigations.

## 5. REFERENCES

[1] Rui Liu, Jinhua Zhang, Guanglai Gao, and Haizhou Li, “Betray oneself: A novel audio deepfake detection model via mono-to-stereo conversion,” *arXiv preprint arXiv:2305.16353*, 2023.

[2] Rui Liu, Jinhua Zhang, and Guanglai Gao, “Multi-space channel representation learning for mono-to-binaural conversion based audio deepfake detection,” *Information Fusion*, vol. 105, pp. 102257, 2024.

[3] Rui Liu, Jinhua Zhang, and Haizhou Li, “Hierarchical multi-source cues fusion for mono-to-binaural based audio deepfake detection,” *Information Fusion*, vol. 120, pp. 103097, 2025.

[4] David Combei, Adriana Stan, Dan Oneaă, and Horia Cucu, “Wavlm model ensemble for audio deepfake detection,” *The Automatic Speaker Verification Spoofing Countermeasures Workshop (ASVspoof 2024)*, 2024.

[5] Emanuele Conti, Davide Salvi, Clara Borrelli, Brian Hosler, Paolo Bestagini, Fabio Antonacci, Augusto Sarti, Matthew C Stamm, and Stefano Tubaro, “Deepfake speech detection through emotion recognition: a semantic approach,” in *ICASSP 2022-2022 IEEE international conference on acoustics, speech and signal processing (ICASSP)*. IEEE, 2022, pp. 8962–8966.

[6] Junyan Wu, Qilin Yin, Ziqi Sheng, Wei Lu, Jiwu Huang, and Bin Li, “Audio multi-view spoofing detection framework based on audio-text-emotion correlations,” *IEEE Transactions on Information Forensics and Security*, 2024.

[7] Kuiyuan Zhang, Zhongyun Hua, Rushi Lan, Yushu Zhang, and Yifang Guo, “Phoneme-level feature discrepancies: A key to detecting sophisticated speech deepfakes,” in *Proceedings of the AAAI Conference on Artificial Intelligence*, 2025, vol. 39, pp. 1066–1074.

[8] Bo Wang, Yeling Tang, Fei Wei, Zhongjie Ba, and Kui Ren, “Ftdkd: Frequency-time domain knowledge distillation for low-quality compressed audio deepfake detection,” *IEEE/ACM Transactions on Audio, Speech, and Language Processing*, 2024.

[9] Klaus R Scherer, “Vocal communication of emotion: A review of research paradigms,” *Speech communication*, vol. 40, no. 1-2, pp. 227–256, 2003.

[10] Wei-Cheng Lin and Carlos Busso, “Sequential modeling by leveraging non-uniform distribution of speech emotion,” *IEEE/ACM Transactions on Audio, Speech, and Language Processing*, vol. 31, pp. 1087–1099, 2023.

[11] Xingfeng Li, Xiaohan Shi, Desheng Hu, Yongwei Li, Qingchen Zhang, Zhengxia Wang, Masashi Unoki, and Masato Akagi, “Music theory-inspired acoustic representation for speech emotion recognition,” *IEEE/ACM Transactions on Audio, Speech, and Language Processing*, 2023.

[12] Rendi Chevi and Alham Fikri Aji, “Daisy-tts: simulating wider spectrum of emotions via prosody embedding decomposition,” *arXiv preprint arXiv:2402.14523*, 2024.

[13] Ruskin Raj Manku, Yuzhi Tang, Xingjian Shi, Mu Li, and Alex Smola, “Emergenttts-eval: Evaluating tts models on complex prosodic, expressiveness, and linguistic challenges using model-as-a-judge,” *arXiv preprint arXiv:2505.23009*, 2025.

[14] Christopher M Bishop and Nasser M Nasrabadi, *Pattern recognition and machine learning*, vol. 4, Springer, 2006.

[15] Alexei Baevski, Henry Zhou, Abdel Rahman Mohamed, and Michael Auli, “wav2vec 2.0: A framework for self-supervised learning of speech representations,” *ArXiv*, vol. abs/2006.11477, 2020.

[16] Wei-Ning Hsu, Benjamin Bolte, Yao-Hung Hubert Tsai, Kushal Lakhotia, Ruslan Salakhutdinov, and Abdel Rahman Mohamed, “Hubert: Self-supervised speech representation learning by masked prediction of hidden units,” *IEEE/ACM Transactions on Audio, Speech, and Language Processing*, vol. 29, pp. 3451–3460, 2021.

[17] Jee-weon Jung, Hee-Soo Heo, Hemlata Tak, Hye-jin Shim, Joon Son Chung, Bong-Jin Lee, Ha-Jin Yu, and Nicholas Evans, “Aasist: Audio anti-spoofing using integrated spectro-temporal graph attention networks,” in *ICASSP 2022-2022 IEEE international conference on acoustics, speech and signal processing (ICASSP)*. IEEE, 2022, pp. 6367–6371.

[18] Ziyang Ma, Zhisheng Zheng, Jiaxin Ye, Jinchao Li, Zhifu Gao, Shiliang Zhang, and Xie Chen, “emotion2vec: Self-supervised pre-training for speech emotion representation,” *ArXiv*, vol. abs/2312.15185, 2023.

[19] Ting Chen, Simon Kornblith, Mohammad Norouzi, and Geoffrey Hinton, “A simple framework for contrastive learning of visual representations,” in *International conference on machine learning*. PMLR, 2020, pp. 1597–1607.

[20] Alex Kendall, Yarin Gal, and Roberto Cipolla, “Multi-task learning using uncertainty to weigh losses for scene geometry and semantics,” in *Proceedings of the IEEE conference on computer vision and pattern recognition*, 2018, pp. 7482–7491.

[21] Massimiliano Todisco, Xin Wang, Ville Vestman, Md Sahidullah, Héctor Delgado, Andreas Nautsch, Junichi Yamagishi, Nicholas Evans, Tomi Kinnunen, and Kong Aik Lee, “Asvspoof 2019: Future horizons in spoofed and fake audio detection,” *arXiv preprint arXiv:1904.05441*, 2019.

[22] Junichi Yamagishi, Xin Wang, Massimiliano Todisco, Md Sahidullah, Jose Patino, Andreas Nautsch, Xuechen Liu, Kong Aik Lee, Tomi Kinnunen, Nicholas Evans, et al., “Asvspoof 2021: accelerating progress in spoofed and deepfake speech detection,” *arXiv preprint arXiv:2109.00537*, 2021.

[23] Zhizheng Wu, Tomi Kinnunen, Nicholas Evans, Junichi Yamagishi, Cemal Hanlıç, Md Sahidullah, and Aleksandr Sizov, “Asvspoof 2015: the first automatic speaker verification spoofing and countermeasures challenge,” in *INTERSPEECH 2015, Automatic Speaker Verification Spoofing and Countermeasures Challenge, colocated with INTERSPEECH 2015*. ISCA, 2015, pp. 2037–2041.

[24] Tomi Kinnunen, Kong Aik Lee, Héctor Delgado, Nicholas Evans, Massimiliano Todisco, Md Sahidullah, Junichi Yamagishi, and Douglas A Reynolds, “t-dcf: a detection cost function for the tandem assessment of spoofing countermeasures and automatic speaker verification,” *arXiv preprint arXiv:1804.09618*, 2018.

[25] Xiaohui Liu, Meng Liu, Longbiao Wang, Kong Aik Lee, Hanyi Zhang, and Jianwu Dang, “Leveraging positional-related local-global dependency for synthetic speech detection,” in *ICASSP 2023-2023 IEEE International Conference on Acoustics, Speech and Signal Processing (ICASSP)*. IEEE, 2023, pp. 1–5.

[26] Bingyuan Huang, Sanshuai Cui, Jiwu Huang, and Xiangui Kang, “Discriminative frequency information learning for end-to-end speech anti-spoofing,” *IEEE Signal Processing Letters*, vol. 30, pp. 185–189, 2023.

[27] Cunhang Fan, Jun Xue, Jianhua Tao, Jiangyan Yi, Chenglong Wang, Chengshi Zheng, and Zhao Lv, “Spatial reconstructed local attention res2net with f0 subband for fake speech detection,” *Neural Networks*, vol. 175, pp. 106320, 2024.

[28] Yinlin Guo, Haofan Huang, Xi Chen, He Zhao, and Yuehai Wang, “Audio deepfake detection with self-supervised wavlm and multi-fusion attentive classifier,” in *ICASSP 2024-2024 IEEE International Conference on Acoustics, Speech and Signal Processing (ICASSP)*. IEEE, 2024, pp. 12702–12706.

[29] Zuheng Kang, Yayun He, Botao Zhao, Xiaoyang Qu, Junqing Peng, Jing Xiao, and Jianzong Wang, “Retrieval-augmented audio deepfake detection,” in *Proceedings of the 2024 International Conference on Multimedia Retrieval*, 2024, pp. 376–384.